Integral colorimeter based on compound LED illumination

Kun Yuan (袁 琨)[1,2*], Huimin Yan (严惠民)[1], and Shangzhong Jin (金尚忠)[2]

[1] *State Key Laboratory of Modern Optical Instrument, Zhejiang University, Hangzhou 310027, China*

[2] *College of Optical and Electronic Technology, China Jiliang University, Hangzhou 310018, China*

[*] *Corresponding author: 10930014@zju.edu.cn*

Received November 15, 2013; accepted December 19, 2013; posted online January 27, 2014

Traditional integral colorimeters use tungsten–halogen or xenon lamps for illumination, as well as correcting filters to make the instrument's spectral response meet the Luther condition. This structure causes the instruments to have relatively higher error and poor repeatability. Thus, this letter proposes a new measurement design that uses compound LEDs as the instrument's measurement light source. The new design adjusts the instrument's spectral response by modifying the spectra of the compound LEDs. A compound LED light source is designed for integral colorimeters, and an experiment is conducted to evaluate the performance of the integral colorimeter. Experiments show that the design effectively reduces the error of integral colorimeters.

OCIS codes: 330.1710, 040.5160, 120.6200.

doi: 10.3788/COL201412.023302.

Integral colorimeters are widely used in areas such as painting[1], medical treatment[2], agriculture[3,4], and plastics[5]. Wang *et al.*[1] used a colorimeter to create a color separation criterion for spectral multi-ink printer characterization. Xiao *et al.*[2] used a colorimeter to investigate Chinese skin color and appearance. Intaravanne *et al.*[3,4] used a mobile device-based application to estimate banana ripeness and analyze the color level of rice leaf for nitrogen estimation. Polyzois *et al.*[5] measured color changes to evaluate the effect of accelerated aging on materials. The spectral response of integral colorimeters is based on the relative spectral sensitivity of the sensor, the illumination spectrum power distribution (SPD), and the spectral transmittance of the filter. Sametoglu *et al.*[6] used a RGB sensor as the colorimeter detector. Shannon *et al.*[7] presented a method of calculating the thickness for the filter matching of a colorimeter.

In integral colorimeters, tungsten–halogen or xenon lamps are often used as the illumination source, and correcting filters are used to make the instrument's spectral response meet the Luther condition. In actual applications, tungsten–halogen lamps have low intensity at the short-wavelength part of the visible spectra, causing the measurement to have a low signal-to-noise ratio (SNR) and reducing the instrument's repeatability. Xenon lamps have non-smooth spectral distribution, and appropriate filters that meet the Luther condition are difficult to find. Moreover, the type of colored glass is limited, and accurately correcting it is difficult (a large error would exist for the instrument). If multiple filters are used, the transmittance would be relatively low, which also lowers the instrument's repeatability. Accordingly, researchers have exerted efforts to improve the accuracy of integral colorimeters using a calibration algorithm. Soloviev *et al*[8] proposed an integral colorimeter that functions according to the principles of ar tificial neural nets. Gardner[9] established a calibration model possessing low chromaticity uncertainties.

This research proposes a new design for integral colorimeters using compound LEDs for illumination. The instrument's spectral response is adjusted by modifying the spectra of the compound LEDs. According to color measurement principles recommended by the international Gommission on illumination (CIE), when measuring the color tristimulus under CIE illuminant D65, the instrument's spectral response should meet

$$\left.\begin{aligned} k_1 \int_{360}^{780} S(\lambda) T_{\mathrm{x}}(\lambda) \gamma(\lambda) \mathrm{d}\lambda = \int_{360}^{780} S_D(\lambda) \overline{x}_{10}(\lambda) \mathrm{d}(\lambda) \\ k_2 \int_{360}^{780} S(\lambda) T_{\mathrm{y}}(\lambda) \gamma(\lambda) \mathrm{d}\lambda = \int_{360}^{780} S_D(\lambda) \overline{y}_{10}(\lambda) \mathrm{d}(\lambda) \\ k_3 \int_{360}^{780} S(\lambda) T_{\mathrm{z}}(\lambda) \gamma(\lambda) \mathrm{d}\lambda = \int_{360}^{780} S_D(\lambda) \overline{z}_{10}(\lambda) \mathrm{d}(\lambda) \end{aligned}\right\}, \tag{1}$$

where k_1, k_2, and k_3 are constants that balance each side of the equation; $S(\lambda)$ is the relative SPD of the instrument light source; $T_{\mathrm{x}}(\lambda), T_{\mathrm{y}}(\lambda)$, and $T_{\mathrm{z}}(\lambda)$ are the spectral transmittance of the filters; $T_{\mathrm{D}}(\lambda)$ is the normalized intensity of CIE illuminant D65, whose SPD is shown in Fig. 1(a); $\overline{x}_{10}(\lambda), \overline{y}_{10}(\lambda)$, and $\overline{z}_{10}(\lambda)$ are the spectral tristimulus of CIE 1964 standard observer, as shown in Fig. 1(b); $\gamma(\lambda)$ represents the sensor's relative spectral response.

The color measurement condition satisfied in Eq. (1) is called the Luther condition. As shown in Eq. (1), the spectral response of the instrument is based on the light source, detector, and filters. After the light source and sensor are determined, the spectrum transmittance of the filters is chosen to meet the Luther condition. Based on Eq. (1), the relative transmittance of the X, Y, Z

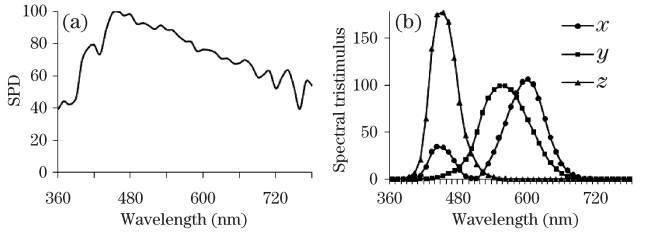

Fig. 1. Color measurement spectra recommended by the CIE: (a) SPD of D65 illuminant and (b) CIE 1964 spectral tristimulus.

filters should satisfy

$$\left.\begin{aligned}\tau_x(\lambda) &= \frac{S_{\mathrm{D}}(\lambda)\overline{x}_{10}(\lambda)}{S(\lambda)\gamma(\lambda)}\\ \tau_y(\lambda) &= \frac{S_{\mathrm{D}}(\lambda)\overline{y}_{10}(\lambda)}{S(\lambda)\gamma(\lambda)}\\ \tau_z(\lambda) &= \frac{S_{\mathrm{D}}(\lambda)\overline{z}_{10}(\lambda)}{S(\lambda)\gamma(\lambda)}\end{aligned}\right\}, \tag{2}$$

where $\tau_x(\lambda)$, $\tau_y(\lambda)$, and $\tau_z(\lambda)$ are the relative spectral transmittance of the filters.

The SPD of the tungsten-halogen lamp is shown in Fig. 2(a). Silicon detectors are usually used as the colorimeter's sensor. They have low response at shortwave lengths, as shown in Fig. 2(b). The needed filter's relative transmittance is shown in Fig. 2(c). When tungsten-halogen lamps are used as the measurement source, the measurement of the Z value is bound to have a low SNR and low repeatability.

Xenon lamps have ample distribution throughout the visible spectra, but their spectra are not smooth, as shown in Fig. 2(d). Thus, filter matching becomes very difficult, as shown in Fig. 2(e).

To solve those problems, this letter proposes to use compound LEDs to measure illumination and adjust the spectral response of the instrument by modifying the output spectra of the compound LEDs. Filters are not used in this design; the instrument's spectral responses are based on the SPD of the LED light sources and spectral response of the detector and should satisfy

$$\left.\begin{aligned}c_1\int_{360}^{780} S(\lambda)L_{T\mathrm{x}}(\lambda)\gamma(\lambda)\mathrm{d}\lambda &= \int_{360}^{780} S_D(\lambda)\overline{x}_{10}(\lambda)\mathrm{d}(\lambda)\\ c_2\int_{360}^{780} S(\lambda)L_{T\mathrm{y}}(\lambda)\gamma(\lambda)\mathrm{d}\lambda &= \int_{360}^{780} S_D(\lambda)\overline{y}_{10}(\lambda)\mathrm{d}(\lambda)\\ c_3\int_{360}^{780} S(\lambda)L_{T\mathrm{z}}(\lambda)\gamma(\lambda)\mathrm{d}\lambda &= \int_{360}^{780} S_D(\lambda)\overline{z}_{10}(\lambda)\mathrm{d}(\lambda)\end{aligned}\right\}, \tag{3}$$

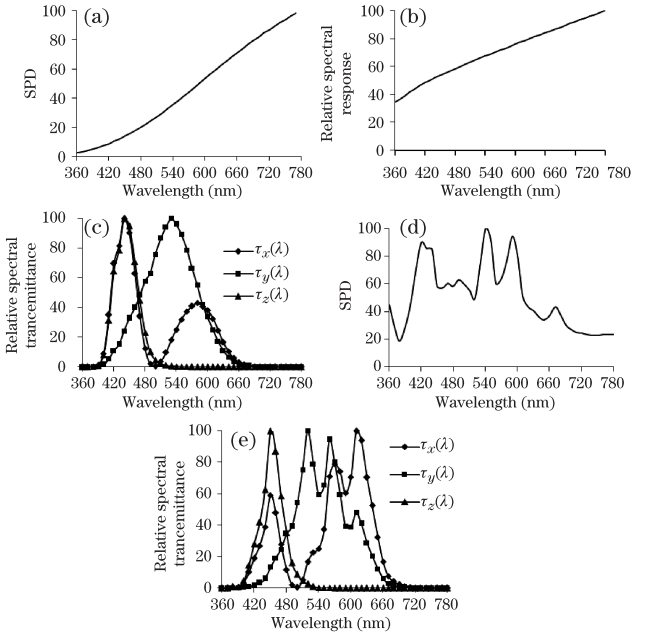

Fig. 2. Filter relative transmittance calculation with tungsten–halogen and xenon lamps: (a) SPD of tungsten–halogen lamp, (b) silicon detector spectrum response, (c) filter transmittance with tungsten–halogen lamp, (d) SPD of xenon lamp, and (e) filter transmittance with xenon lamp.

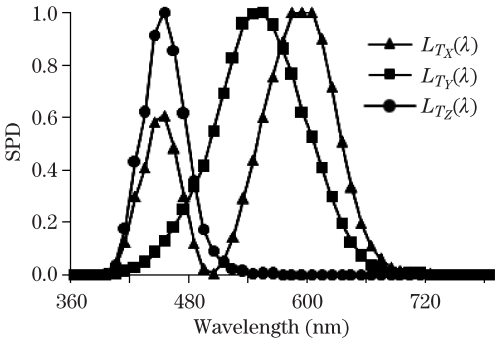

Fig. 3. Target SPD of compound LEDs.

where $L_{Tx}(\lambda)$, $L_{Ty}(\lambda)$, and $L_{Tz}(\lambda)$ are the target SPD of the compound LEDs when measuring tristimulus values X, Y, and Z; c_1, c_2, and c_3 are constants. Using a sensor whose spectral response is as shown in Fig. 2(b), $L_{Tx}(\lambda)$, $L_{Ty}(\lambda)$, and $L_{Tz}(\lambda)$ are obtained (Fig. 3).

In this research, 31 LEDs are used in the compound LEDs. By modifying the driving current of the LEDs, three different compound light sources are designed. More LEDs and smaller intervals between peak wavelengths result in better fitting accuracy but are limited by cost, instrument structure, and LED type. Thus, in the design of this instrument, LEDs are chosen with intervals between peak wavelengths of 10–15 nm.The peak wavelengths of the 31 LEDs are 400, 412, 424, 436, 448, 460, 472, 484, 496, 508, 520, 532, 544, 556, 568, 580, 592, 604, 616, 628, 640, 654, 668, 678, 692, 711, 727, 740, 752, 765, and 780 nm. Considering that the LED with peak wavelength at 400 nm has a half spectral width of 20 nm, it can provide the intensity distributed at 380 nm. The spectral tristimulus value of CIE 1964 at 360 and 370 nm is zero. Thus, LEDs with peak wavelengths at 360, 370, 380, and 390 nm were not included.

Based on spectral superposition principles, the fitting model of the LED compound light source is expressed[10] as

$$L_i(\lambda) = \Sigma_{j=1}^{n} S_j(\lambda) \times K_{ij}, \tag{4}$$

where i is the type of compound LEDs X, Y, and Z; K_{ij} is the driving current coefficient of the jth LED; $S_j(\lambda)$ is the SPD of the jth LED; n is the number of LEDs. The following equation evaluates the consistency between the actual SPD of compound LEDs $L_i(\lambda)$ and the target SPD of $L_{Ti}(\lambda)$. When the minimum value is reached, $L_i(\lambda)$ is the closest to the $L_{Ti}(\lambda)$, and then the optimized K_{ij} can be obtained.

$$\Sigma|L_{Ti}(\lambda) - L_i(\lambda)| = \min. \tag{5}$$

Relative error used to evaluate the consistency between $L_i(\lambda)$ and $L_{Ti}(\lambda)$[11,12] is calculated by

$$f_1' = \frac{\Sigma|L_{Ti}(\lambda) - L_i(\lambda)|}{\Sigma L_{Ti}(\lambda)}, \tag{6}$$

where f_1' is the fitting accuracy, and a lower f_1' corresponds to a higher spectral consistency between $L_i(\lambda)$ and $L_{Ti}(\lambda)$. According Eq. (4), the optimized K_{ij} can be calculated by

$$\boldsymbol{L_{Ti}} = \boldsymbol{S} \times \boldsymbol{K}_i, \tag{7}$$

where

$$\boldsymbol{L_{Ti}} = [L_{Ti}(360)L_{Ti}(370)L_{Ti}(380)\cdots L_{Ti}(780)]^{\mathrm{T}},$$

$$\boldsymbol{S} = \begin{bmatrix} S_1(360) & S_2(360)\cdots S_n(360) \\ S_1(370) & S_2(370)\cdots S_n(370) \\ \vdots & \vdots \quad \ddots \quad \vdots \\ S_1(380) & S_2(380)\cdots S_n(380) \end{bmatrix},$$

$$\boldsymbol{K}_1 = [K_{i1}K_{i2}K_{i3}\cdots K_{in}]^{\mathrm{T}}.$$

The optimized solution for matrix K_i can be obtained through multi-variable linear regression. A Matlab program is used for the calculation. The experiment results for the SPD of the three compound LED light sources $L_x(\lambda)$, $L_y(\lambda)$, and $L_z(\lambda)$, are shown in Fig. 4. The fitting accuracy f_1' in the actual experiment is shown in Table 1.

Table 1. Spectral Fitting Evaluation

Light Source	f_1' Value
L_x	0.037
L_y	0.035
L_z	0.049

Using the prepared compound LED light source, an integral colorimeter is subsequently designed.The structure of the design uses a D/8 illumination structure; the 31 perforation holes are uniformly distributed on the inner surface of the integrating sphere that is parallel to the surface of the measured object, as shown in Fig. 5(a). The compound LED light source consists of 31 LEDs; light from each LED enters the sphere through a perforation hole. Figure 5(b) is the vertical view of the middle section of the integrating sphere. The sensor is on the inner surface of the integrating sphere 8° from the normal of the sample. Light from the light source firstly illuminates the inner surface of the integrating sphere and provides diffused illumination to the sample, and then the sensor collects light signal and transmits it to the computer for measurement.

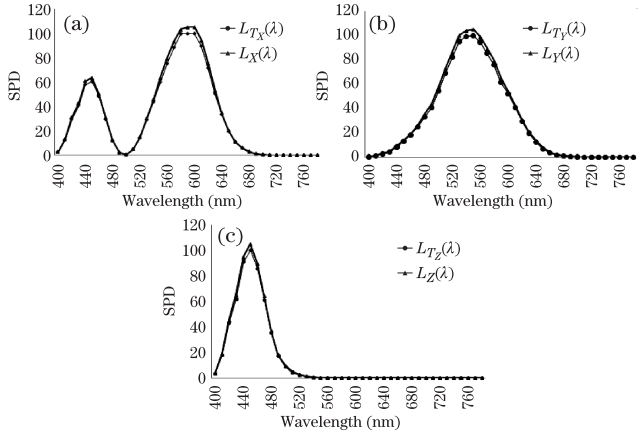

Fig. 4. Comparison between target SPD and experimental results of compound LED light source: (a) between $L_{TX}(\lambda)$ and $L_X(\lambda)$, (b) between $L_{TY}(\lambda)$ and $L_Y(\lambda)$, and (c) between $L_{TZ}(\lambda)$ and $L_Z(\lambda)$.

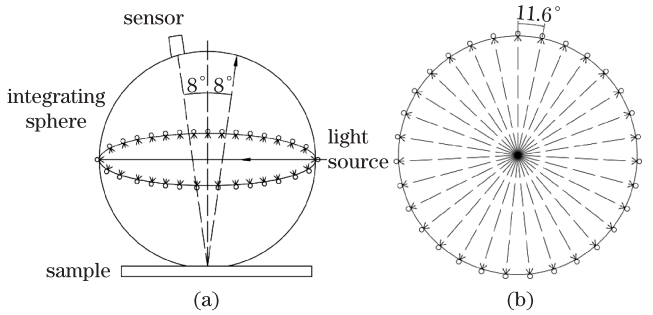

Fig. 5. Structure of integral colorimeter with a LED compound light source: (a) measurement structure and (b) arrangement of compound LED light source.

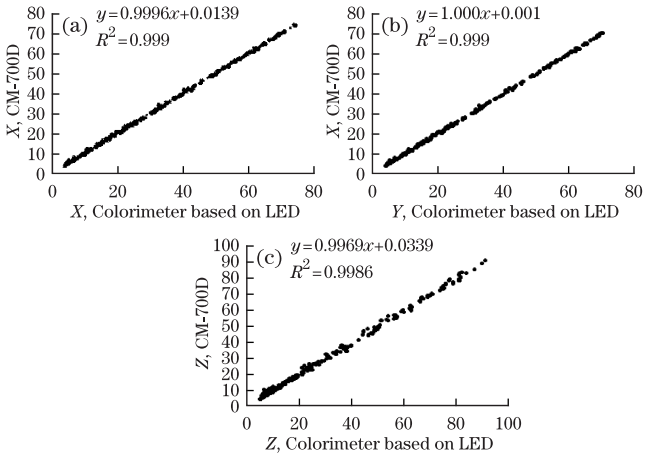

Fig. 6. Comparison of (a) X, (b) Y, and (c) Z value test results with those using optimized and standard instruments.

The instrument shown in Fig. 5 and a standard instrument are used to measure the sample. The standard instrument used is Konica Minolta spectrophotometer CM-700D, which can measure the reflective spectra of the sample and provide tristimulus values of the sample illuminated by standard light sources. The samples are 224 Pantone-C color charts. The experiment results shown in Fig. 6 indicate that the findings from the two instruments have good relativity for all three tristimuli (X, Y, and Z), with Y having better relativity than X and Z. After calibrating the instrument structure using the results from the CM-700D instrument, BCRA standard color charts are measured using the instrument, and the results are shown in Table 2. According to JJG595-2002[13], the performance of the integral colorimeter could be evaluated by testing the BRCA-compared test data with standard data. (x, y) is the color coordinate calculated by

$$\left.\begin{aligned} x &= \frac{X+Y+Z}{X} \\ y &= \frac{X+Y+Z}{X} \end{aligned}\right\}. \tag{8}$$

The experimental results show that the integral colorimeter using the compound LED light source meets the measurement requirements of first-class colorimeters.

In conclusion, this letter uses compound LEDs as an illumination source and acquires the required spectral distribution by modifying the driving currents of the 31 LEDs. The measurement results from the new design are

Table 1. BCRA Test Data

	Standard Data			Test Data			D-Value		
	Y	x	y	Y	x	y	Y	Δx	Δy
BCRA-BLK	4.81	0.3098	0.3290	4.72	0.3124	0.3294	−0.09	0.0025	0.0004
BCRA-YELL	62.84	0.4518	0.4656	62.23	0.4498	0.4644	−0.61	−0.0020	−0.0012
BCRA-DFGRY	28.29	0.3130	0.3314	28.17	0.3128	0.3311	−0.12	−0.0002	−0.0003
BCRA-RED	15.12	0.4736	0.3350	15.10	0.4688	0.3349	−0.02	−0.0048	0.0000
BCRA-WHT	89.44	0.3185	0.3366	88.77	0.3171	0.3350	−0.67	−0.0015	−0.0016
BCRA-ORAN	35.88	0.5055	0.3874	35.41	0.5019	0.3864	−0.47	−0.0036	−0.0010
BCRA-MDGRY	27.71	0.3112	0.3374	27.59	0.3111	0.3372	−0.12	−0.0001	−0.0002
BCRA-DKGRY	9.13	0.3155	0.3322	9.10	0.3160	0.3321	−0.03	0.0005	−0.0001
BCRA-DFGRN	24.29	0.3004	0.4094	24.31	0.3004	0.4104	0.02	0.0001	0.0010
BCRA-CYAN	24.59	0.2203	0.2686	24.69	0.2208	0.2706	0.10	0.0005	0.0020
BCRA-DBLUE	5.67	0.2587	0.2381	5.70	0.2588	0.2376	0.03	0.0001	−0.0006
BCRA-DROSE	15.02	0.3761	0.3107	14.90	0.3749	0.3100	−0.12	−0.0012	−0.0007
BCRA-DFGRN	23.61	0.2923	0.4019	23.71	0.2927	0.4029	0.10	0.0004	0.0009

compared with those from a standard colorimeter. The tristimulus results X, Y, and Z from the two instruments show good relativity. Results from measuring BCRA color charts show that this design effectively reduces the indicating error of integral colorimeters. The indicating error mainly originates from the fitting error of the compound LED light source and the difference of the light source's actual spectra from the ideal simulated spectra. The fitting could be improved in future work.

This work was supported by the Chinese National Programs for Scientific Instruments Research and Development (No. 2011YQ03012403), the Program of General Administration of Quality Supervision, Inspection and Quarantine of China (No. 201210094), and the Zhejiang SSL Science and Tech Innovation Team Funded Project (No. 2010R50020).

References

1. B. Wang, H. Xu, and M. Luo, Chin. Opt. Lett. **10,** 013301 (2012).
2. K. Xiao, N. Liao, F. Zardawi, H. Liu, R. Van Noort, Z. Yang, M. Huang, and J. Yates, Chin. Opt. Lett. **10,** 083301 (2012).
3. Y. Intaravanne, S. Sumriddetchkajorn, and J. Nukeaw, Sensor. Actuator. B: Chem. **168,** 390 (2012).
4. Y. Intaravanne and S. Sumriddetchkajorn, Proc. SPIE **8558,** 85580F (2012).
5. G. Polyzois, I. Kostoulas, D. Nikolovieni, A. Mitsoudis, and M. Frangou, Odontology **101,** 193 (2013).
6. F. Sametoglu and O. Celikel, MAPAN-Journal of Metrology Society of India **27,** 149 (2012).
7. C. Shannon, D. Slocum, and M. Vrhel, "Method for Designing a Colorimeter having Illuminant-Weighted CIE Color-Matching Filters" U.S.Patent US7580130B2 (2009).
8. V. A. Soloviev and M. N. Morozova, Measurement Techniques **55,** 914 (2012).
9. J. L. Gardner, Color Res. Appl. **38,** 251 (2013).
10. I. Fryc, S. W. Brown, G. P. Eppeldaure, and Y. Ohno, Proc. SPIE **5530,** 150 (2004).
11. I. Fryc, S. W. Brown, and Y. Ohno, Proc. SPIE **5941,** 59411I (2005).
12. JJG245-2005, "Illuminance Meter". China: General Administration of Quality Supervision, Inspection and Quarantine of the People's Republic of China (2005).
13. JJG595-2002, "Colorimeter and color difference meter". China: General Administration of Quality Supervision, Inspection and Quarantine of the People's Republic of China (2002).